Anomalous coalescence in sheared two-dimensional foam

Hadi Mohammadigoushki,[1] Giovanni Ghigliotti,[1] and James J. Feng[1,2]
[1]*Department of Chemical and Biological Engineering, University of British Columbia, Vancouver, British Columbia, V6T 1Z3 Canada*
[2]*Department of Mathematics, University of British Columbia,Vancouver, British Columbia, V6T 1Z2 Canada*
(Received 13 August 2011; revised manuscript received 15 May 2012; published 1 June 2012)

We report an experimental study on shearing a monolayer of monodisperse bubbles floating on liquid in a narrow-gap Couette device. The bubbles in such a "bubble raft" coalesce only if the shear rate exceeds a threshold value. This is in contrast to the conventional wisdom that bubbles and drops coalesce for gentler collisions, at shear rates below a critical value. Furthermore, the threshold shear rate increases with the bubble size and the viscosity of the suspending liquid, contravening reasoning based on capillary number. Through visualization and scaling arguments, we investigate several plausible mechanisms for the anomalous coalescence. None explains all aspects of the observations. The most promising model is one based on inertial forces that compress the bubbles radially inward and accelerate film drainage.

DOI: 10.1103/PhysRevE.85.066301 PACS number(s): 47.55.dd, 47.55.df, 47.57.Bc

I. INTRODUCTION

Foams are fragile soft matter, with a microstructure that tends to evolve under interfacial, hydrodynamic, and body forces. Even a static foam may undergo several types of structural changes. Coarsening occurs when gas diffuses from a smaller bubble to a larger neighbor [1]. Bubbles burst at the interface with free air as the liquid film is depleted by drainage or evaporation [2,3]. In the interior of a static dry foam, liquid drainage may lead to neighbor-swapping T1 events [4], which in turn may cause bubble coalescence [5,6].

Shearing opens up dynamic routes for structural evolution. T1 events are prominent under shear [7,8]. Golemanov *et al.* [9] observed breakup of bubbles sheared between parallel disks. In a similar geometry, Herzhaft [10] reported size-based segregation of bubbles in a polydisperse foam. Smaller bubbles tend to aggregate near the top and bottom plates, while larger ones tend to aggregate in the middle. Conspicuously missing, however, is any report of *shear-induced coalescence*, a common occurrence in sheared emulsions [11]. This has motivated the current experiment on bubble-bubble coalescence in a sheared foam.

A severe limitation to understanding the structure-flow coupling in a three-dimensional (3D) foam comes from its intrinsic opacity; the myriad gas-liquid interfaces diffract light. Therefore, researchers have experimented with *2D foams*, i.e., monolayers of 3D bubbles. Experiments on shearing 2D foams have been carried out in parallel-plate (e.g., [12,13]) and Couette devices (e.g., [8,13,14]), focusing mainly on low shear rates. The only structural changes observed so far are T1 events [8]. We aim to explore structural changes in 2D foams under more vigorous shearing. The main finding is a type of bubble coalescence unexpected at the start. We consider several models for the anomalous coalescence, none of which quantitatively explains all aspects of the observations.

II. MATERIALS AND METHODS

The experiments are carried out in a modified Couette device modeled after that of Ref. [15]. It consists of a stationary outer cylinder of inner radius $R_2 = 10$ cm and a rotating sharp-edged inner disk of radius $R_1 = 9.3$ cm [Fig. 1(a)]. The static liquid level is flush with the top surface of the inner and outer cylinders such that the interface is pinned at the sharp corners. Upon rotation, this limits the undulation of the free surface to the order of 0.1 mm. Furthermore, triangular teeth (height 0.5 mm and width 1 mm) are machined onto the solid surfaces to prevent slippage. Figure 1(b) shows that the innermost and outermost layer of bubbles are essentially entrapped in these dents. Bubbles are produced by blowing nitrogen through an immersed needle in a soapy water solution using a pneumatic PicoPump (WPI, model PV-820). This method allows for an extremely uniform bubble size that can be fine-tuned by the nitrogen pressure. The results reported below are for three bubble sizes, with radius $R = 250$, 350 and 500 μm. Once the bubbles appear to cover the entire liquid surface, relatively few additional bubbles can be squeezed into the foam. Further addition causes bubbles to pile on top of others and destroy the two dimensionality. This limits us to relatively wet 2D foams with modest bubble deformation [Fig. 1(b)].

The suspending solution is made of distilled water, various concentrations of glycerine (Fisher Scientific), and a dishwashing liquid (Unilever, Sunlight); the compositions of the three sample liquids used are given in Table I. All are Newtonian, and their viscosity μ is controlled by the amount of glycerine and measured by a rheometer (Malvern, Kinexus). The surface tension σ, measured by a tensiometer (Cole-Parmer, Surface Tensiomat 21), is shown in Fig. 2 for a range of the bulk detergent concentration c. Similar results are obtained for different glycerine concentrations. Such data suggest a critical micelle concentration, CMC $\approx 0.05\%$, above which σ no longer changes with c. In our experiment, c is dictated by the need to produce stable bubbles that do not burst within the time of experiments (up to 60 min). The lowest permissible concentration is $c \approx 0.5\%$, well above the CMC. The results presented below are for $c = 5\%$.

In a separate experiment, we measured the rising speed of small bubbles with diameter below 1 mm in our soap solutions. The results indicate a velocity consistent with the Stokes formula for a rigid sphere, rather than the Hadamard formula for a spherical bubble [16]. For example, a bubble

 ©2012 American Physical Society

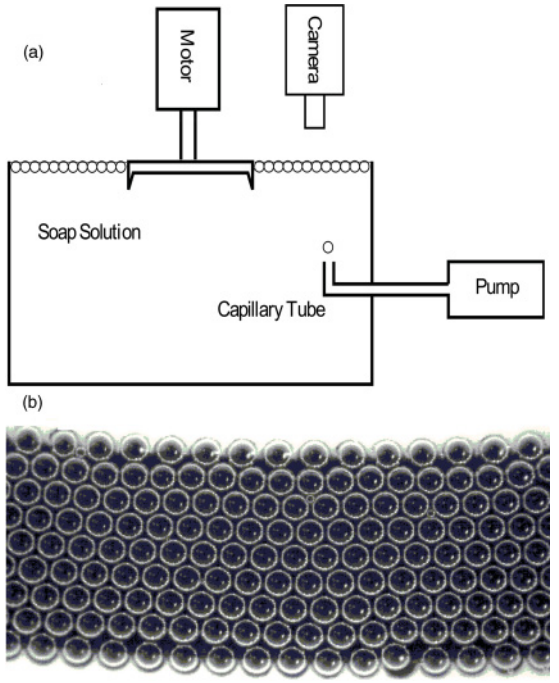

FIG. 1. (a) Schematic of the shear cell (not to scale). (b) A 2D foam at rest with bubble radius $R = 500\ \mu$m.

of radius $R = 450\ \mu$m rises at a speed of $V = 0.018$ m/s, giving a Reynolds number of $\mathrm{Re} = 0.38$. Theoretically, the Stokes formula predicts $V = 0.021$ m/s, while the Hadamard formula would have given $V = 0.032$ m/s. Therefore, the bubble surface is completely immobilized, and the interfacial dynamics is not affected by the surfactant concentration.

The bubble raft is sheared by rotating the inner cylinder. The foam structure is captured with a high-speed camera (Megaspeed, MS 70 K) at 4600 fps. The bubble velocity profile across the gap is measured by a type of particle image velocimetry (PIV) that tracks the bubble position in consecutive exposures and calculates the bubble velocity via image analysis. Typical profiles are shown in Fig. 3. If scaled by the inner wall velocity, the profiles collapse for all Ω and R tested. The bubble velocity falls below the theoretical profile for a Newtonian fluid. Therefore, the foam behaves as a shear-thinning liquid. With increasing μ, the profiles tend to approach that of the Newtonian fluid. Using the measured shear rate $\dot{\gamma}$ at the inner cylinder, we can define a capillary number $\mathrm{Ca} = \mu\dot{\gamma}R/\sigma$. The range of rotational speed of the inner cylinder, $0.05 \leqslant \Omega \leqslant 85$ rpm, thus corresponds to $10^{-6} \leqslant \mathrm{Ca} \leqslant 3 \times 10^{-3}$. Even our largest Ca falls well below the minimum needed for bubble breakup [9]. Indeed, breakup into smaller bubbles or burst never happened under our experimental conditions.

TABLE I. Composition and properties of the solutions.

Solution	Glycerin	c	μ (mPa s)	σ (mN/m)
I	10 wt. %	5 wt. %	1.0 ± 0.1	27.0 ± 1.0
II	30 wt. %	5 wt. %	1.8 ± 0.2	27.0 ± 1.0
III	50 wt. %	5 wt. %	4.2 ± 0.4	27.0 ± 1.0

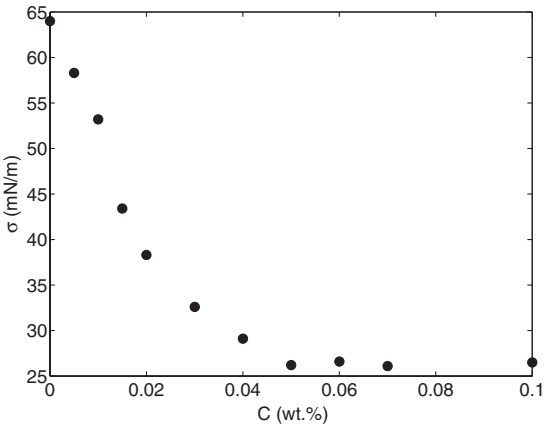

FIG. 2. Surface tension as a function of the concentration of dishwashing liquid, with 30 wt. % glycerine.

III. EXPERIMENTAL RESULTS

A. Critical rotational velocity for bubble-bubble coalescence

The key finding of this study is that above a critical rotational velocity Ω_c, large bubbles appear quickly after the start of shearing (Fig. 4). At shear rates below Ω_c, no large bubble appears and the foam morphology remains unchanged over long periods of time ($\sim$30 min). The threshold is observed for all bubble sizes, liquid compositions, and surfactant concentrations that we tested.

Our optical setup offers a 2×2 cm viewing window that is fixed in space. Thus, we capture only a small portion of the circular trajectory of the bubbles. The coalescence takes place very quickly after shearing above Ω_c. Therefore, we cannot capture the actual process of the coalescence as Ritacco *et al.* [3] did for bursting of bubbles in static bubble raft. Coalescence is thus inferred from the appearance of large bubbles.

This surprising result contravenes the conventional wisdom that coalescence happens for gentler collisions, with an *upper* bound on the shear rate and a corresponding maximum capillary number (e.g., [17–21]). The coalescence between two freely suspended bubbles or drops is governed by the

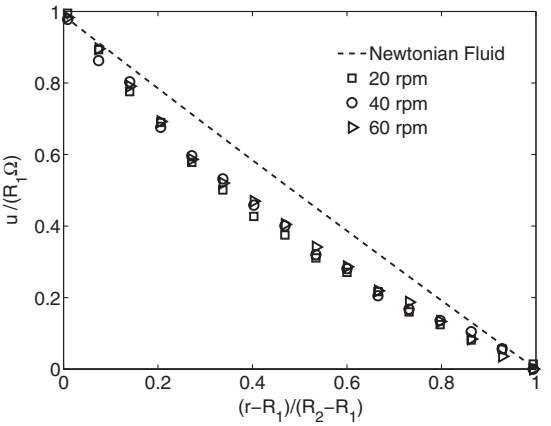

FIG. 3. Bubble velocity profiles at three rotation speeds with liquid I. Bubble size $R = 250\ \mu$m. The line represents the analytical solution for a Newtonian fluid.

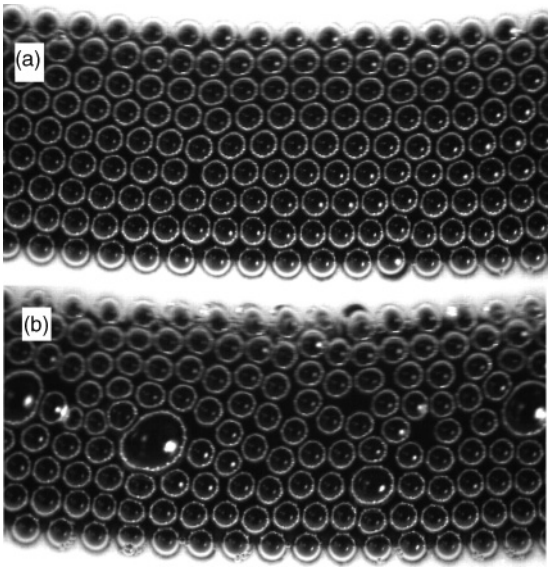

FIG. 4. (a) A foam with bubble radius $R = 500$ μm in liquid I shows no sign of coalescence when sheared at 60 rpm. (b) Large bubbles appear after about 20 sec of shearing at 75 rpm.

competition between two time scales, i.e., the interaction time t_i and the drainage time t_d. The former is the time available for the two bubbles to interact, and scales with $\dot{\gamma}^{-1}$, while the latter is the time required for the liquid film between them to drain to a critical thickness such that van der Waals forces can effect a rupture [19]. Therefore, t_d increases with the viscosity of the suspending liquid and the extent of bubble deformation. The requirement of $t_i \gtrsim t_d$ for coalescence leads to an upper critical capillary number. Such a criterion has been verified by extensive studies that examined various parameters in the process, including drop size, viscosity of the fluids, lateral offset of the colliding drops, and surfactant concentration (e.g., [22,23]). But apparently it does not apply in our case.

B. Effect of bubble size and liquid viscosity

To probe our *anomalous* coalescence, we have examined the effects of the bubble size R and liquid viscosity μ. Figure 5 shows that the critical angular velocity Ω_c increases with both R and μ. This may again be surprising: it implies that the anomalous coalescence cannot be analyzed in the conventional framework of a capillary number, i.e., in terms of viscous forces competing with surface tension. There must be a mechanism at play that was absent in the convention scenario of collision and coalescence.

If we draw straight lines through the data points in this log-log plot, their slopes give the scaling $\Omega_c \sim R^{0.27\pm0.02}$. The dependence of Ω_c on the liquid viscosity μ is rather weak: $\Omega_c \sim \mu^{0.1}$.

C. Interfacial shape and bubble distribution

Aside from bubble-bubble coalescence, we have also recorded the shape of the foam-air interface and spatial

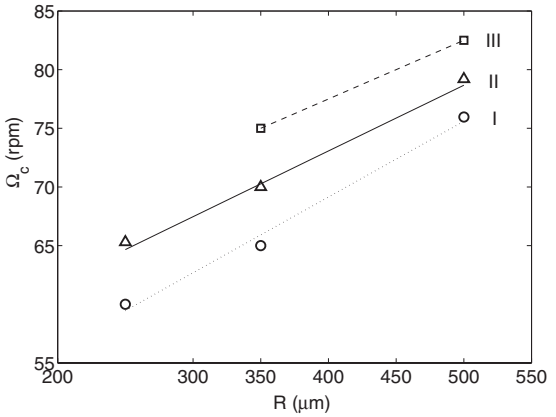

FIG. 5. Critical rotation speed Ω_c as a function of bubble radius R for liquids I, II, and III (see Table I).

redistribution of the bubbles under shear. These may offer potential clues to the cause of the anomalous coalescence.

Intuitively, one may expect the centripetal force to deform the interface on the rotating liquid. This is not the case; the interface exhibits no observable variation in its elevation across the gap even at the highest Ω tested. This is largely due to pinning of the interface at the solid walls. In the experiment, we fill the gap between the cylinders such that the static liquid surface is flush with the tops of the cylinders. Once shearing starts, the free surface is subject to the centripetal force as well as anchoring (i.e., Gibbs pinning) on the sharp edges of the inner and outer walls. Using the velocity profiles of Fig. 3, we have computed the shape of the interface, shown in Fig. 6 for a rotational speed of 60 rpm. Thus, the anchoring of the surface limits its undulation to negligible amounts (<0.2 mm; one order of magnitude smaller than without anchoring). The radial pressure gradient due to centripetal force is maintained by the capillary force in the meniscus rather than the hydrostatic head of the liquid. Furthermore, the bubbles are held mostly underwater by surface tension [24,25].

At relatively low rotation speed, the bubbles slide past each other in rows. At higher Ω, however, there appears to be radial motion of the bubbles that disrupts the layers. As a result, bubbles tend to be more tightly packed in the inner half of the gap than in the outer half. In fact, voids of clear liquids start to appear in the outer region (Fig. 7), which quickly disappear after the shearing stops. The most plausible cause of this spatial inhomogeneity is the centripetal force exerted by the rotating

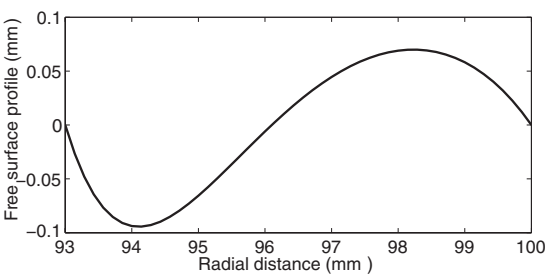

FIG. 6. Shape of the free surface for liquid sheared at $\Omega =$ 60 rpm. The radial distance is measured from the axis of rotation, and the inner and outer boundaries are at 93 and 100 mm, respectively.

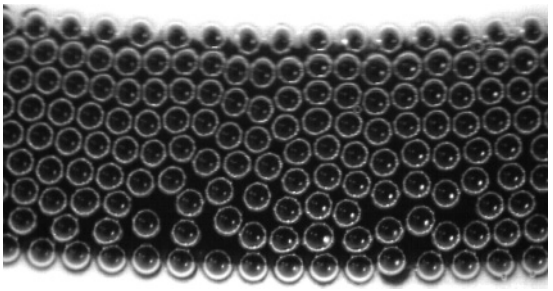

FIG. 7. Bubble distribution in a foam 10 min after shearing at $\Omega = 60$ rpm. $R = 500\ \mu$m.

liquid on the bubbles. As mentioned above, the bubbles are mostly submerged and thus feel an inward force due to the radial pressure gradient in the liquid. This may be a crucial factor in the anomalous coalescence, as explained below.

IV. POTENTIAL MECHANISMS FOR ANOMALOUS COALESCENCE

To rationalize our experimental observation, one first recognizes the differences between our flow situation and that of conventional drop- or bubble-coalescence experiments, from which the conventional wisdom of an upper critical Ca for coalescence has arisen. In shear-induced drop collision, the shear brings into contact two freely suspended drops that would otherwise not interact with each other at all. In our bubble raft, on the other hand, bubbles are in close contact with each other even without shear. Why should the static bubbles be immune to coalescence while the sheared ones are not? Moreover, our bubbles are covered by surfactants, and there is also ample supply of it in the surrounding liquid. Possibly surfactant transport and Marangoni stress have played a part [26]. Finally, our coalescence occurs at relatively high flow rates, much higher than typical for drop-coalescence experiments [26]. In the following, we will explore these differences for clues to the anomalous coalescence.

A. Shear precludes surfactant-stabilized films

The first idea is to explore the contrast between the remarkable stability of static foam and the coalescence in a sheared one. Static foams are stabilized by surfactants because the latter form regular structures in liquid films that are sufficiently thin [27]. If the bulk surfactant concentration is below CMC, then bilayers of surfactants form the so-called "black films" [28]. At higher concentrations, micelles arrange themselves into a more or less regular colloidal structure in the liquid film, producing thick stable films [27]. In either case, the surfactant structure contributes a disjoining pressure that prevents liquid drainage and stabilizes the static foam. Conceivably, vigorous shearing may disrupt such surfactant structures or prevent them from forming in the first place. This could be a mechanism for the observed coalescence.

In a recent study, Denkov *et al*. [29] demonstrated how the black film may cause jamming in flowing foams. In essence, they assume that for low enough shear rates, there is enough time for the film between neighboring bubbles to thin down to a critical thickness where attractive forces act to produce black films. Then the bubbles are locked into a rigid structure that resists the shearing, and the foam is jammed. In our experiment, the surfactant concentration is above CMC and the stable structure should be the thick stable film instead of the black film [27]. At low Ω, we observe nonhomogeneous shearing with large domains of jammed bubbles. Around $\Omega = 3$ rpm, all such domains unjam and the bubble raft starts to shear more or less uniformly. We thus take this to be the threshold for the destruction of the thick stable films. However, larger bubbles only start to appear at a much higher rotational speed of $\Omega \sim 60$ rpm. Therefore, the unjamming cannot be the cause of the anomalous coalescence, which requires much more vigorous shearing.

B. Surface remobilization due to surfactant transport

Aside from forming stable structures in thin films, surfactants also tend to stabilize static foam through the Marangoni effect. Drainage in liquid films carries surfactants along the interface, and creates a spatial gradient in surfactant concentration along the interface of bubbles. This in turn produces a tangential Marangoni stress that resists the interfacial flow. Thus, the bubble surface can be immobilized, as our rising-bubble test has demonstrated. However, the magnitude of the Marangoni stress is limited by the maximum surface concentration gradient that can be produced. Conceivably, sufficiently strong shearing may produce a viscous stress τ_v that overpowers the Marangoni stress τ_M, thereby remobilizing the bubble surfaces. Then film drainage will be facilitated and so will coalescence. This suggests using the Marangoni number $\mathrm{Ma} = \tau_M/\tau_v \sim 1$ as a criterion for the observed anomalous coalescence. In studying pairwise collision of surfactant-covered drops, Yoon *et al*. [26] used this argument to rationalize the appearance of a "transition capillary number" for lower bulk surfactant concentrations such that coalescence occurs *above* it but not below. This seems to be consistent with our anomalous coalescence.

Therefore, we will study the antagonism between Marangoni stress and viscous stress as a potential explanation for the anomalous coalescence observed in our experiment. For soluble surfactants, the surface concentration is determined by two steps: bulk diffusion of surfactants toward the interface and adsorption onto the interface [30]. For our commercial detergent, it is not possible to estimate the relative rates of these two steps. We will examine the cases of either one being the limiting step by adapting the classical analysis of Levich on falling drops [30]. In our problem, the liquid flow outside the bubbles is due to shear instead of sedimentation. Thus, we need to replace the characteristic liquid velocity in Levich's calculations by $\dot{\gamma} R$, with $\dot{\gamma}$ being the local shear rate.

If adsorption is the limiting step that dictates the surfactant distribution Γ on the bubble surface, then one can estimate the surface concentration gradient as [30]

$$|\nabla \Gamma| \approx \frac{\Gamma_0 \dot{\gamma}}{\alpha R}, \tag{1}$$

where Γ_0 is the equilibrium concentration and α is the coefficient of adsorption. This implies that the Marangoni stress,

$$\tau_M = |\nabla \sigma| = \left(\frac{\partial \sigma}{\partial \Gamma}\right)_{\Gamma_0} |\nabla \Gamma|, \tag{2}$$

is proportional to the shear rate. Since the shear stress τ_v on the surface is also proportional to $\dot{\gamma}$, the ratio τ_M/τ_v will be independent of the shear rate. This cannot explain the fact that coalescence happens above a threshold rotational speed.

When the bulk diffusion determines the surfactant distribution on the bubble surface, Levich [30] estimated $|\nabla\Gamma|$ and hence $|\nabla\sigma|$ based on a boundary layer thickness of $\delta \sim (DR/\dot{\gamma})^{1/3}$, with D being the bulk diffusivity:

$$\tau_M = |\nabla\sigma| \approx \frac{\Gamma_0 \dot{\gamma}\delta}{DR}\left(\frac{\partial\sigma}{\partial c}\right). \tag{3}$$

Here, c is the bulk concentration of the surfactant, and $\partial\sigma/\partial c = \Gamma_0 R_g T/c$ by virtue of the Gibbs equation, with R_g and T being the gas constant and absolute temperature, respectively. Now the stress ratio can be written as

$$\frac{\tau_M}{\tau_v} \approx \frac{\Gamma_0^2 R_g T}{c}\frac{\delta}{\mu DR}. \tag{4}$$

From the Stokes-Einstein relationship, the surfactant diffusivity D is inversely proportional to the liquid viscosity μ: $D = k_B T/(6\pi\mu r_s)$, where r_s is the characteristic size of the surfactants and k_B is the Boltzmann constant. By plugging this and the estimation of δ into the above equation, we obtain

$$\frac{\tau_M}{\tau_v} \approx C\,(\mu\dot{\gamma}R^2)^{-1/3}, \tag{5}$$

where C contains factors including T and c, and is a constant in our experiment. The prediction that τ_M/τ_v decreases with $\dot{\gamma}$ allows the possibility that the Marangoni stress is overpowered by the viscous shear stress at sufficiently high $\dot{\gamma}$, which would be consistent with the proposed mechanism of bubble-surface remobilization. However, the prediction of a critical shear rate that scales with μ^{-1} and R^{-2} contradicts the observations in Fig. 5.

In view of the above analysis, we are driven to the conclusion that the remobilization of bubble surface by shear stress overcoming Marangoni stress cannot be the cause of the anomalous coalescence.

C. Bubble compression due to inertia

The photo in Fig. 7 indicates a tendency for the bubbles to be pushed radially inward. The only plausible agent for such an effect is the centripetal force of the rotating liquid. As the spinning liquid generates an inward pressure gradient, the bubbles, having a much lower density than the liquid, are pushed inward towards the inner cylinder. Thanks to pinning on the walls, the liquid surface rises little (Fig. 6). The radial pressure gradient is thus maintained not by hydrostatic head but by surface tension in the liquid meniscus. Conceivably, the squeezing between bubbles accelerates the drainage in the liquid film. If the film drains down to a critical thickness within the interaction time between two bubbles, then coalescence occurs [19]. Thus, one may be able to adapt ideas from a conventional drop-drop collision to explain the anomalous coalescence. In the following, we test this mechanism through a scaling model.

For a pair of bubbles pushed into each other by a constant force F, we may estimate the drainage time from an initial film thickness of h_0 to the final critical one of h_c using the rigid parallel disk model [19,31]:

$$t_d = \frac{3\pi\mu a^4}{4F}\left(\frac{1}{h_c^2} - \frac{1}{h_0^2}\right), \tag{6}$$

where a is the radius of the liquid film. In our geometry, the radial pressure gradient due to the spinning liquid is $dp/dr = \rho u^2/r$, where ρ is the liquid density and u is the tangential velocity of the liquid at distance r. This exerts a force $(dp/dr)(2R)(\pi R^2)$ on each bubble. Since the bubbles are in close contact with each other, they transmit the centripetal force onto their inner neighbors in a sort of force chain, resulting in the largest cumulative force on the innermost layer of bubbles,

$$F = 2\pi\rho R^3 \sum_{i=1}^{N-1}\frac{u^2}{r}, \tag{7}$$

with the summation over the outer layers of bubbles. In comparison with F, the squeezing force $\pi a^2(\sigma/R)$ due to capillary pressure is at least an order of magnitude smaller, and has thus been neglected.

Chesters and Bazhlekov [32] have proposed an empirical relation for the critical film thickness h_c for rupture due to van der Waals force,

$$h_c = \frac{2}{3}\left(\frac{A}{4\pi\sigma}\right)^{0.3}(aR)^{0.2}, \tag{8}$$

with A being the Hamaker constant taken here to be $A = 3\times10^{-19}$ J [33]. We need now to estimate a. For pairwise collisions in a shear flow, the classical theory gives $a/R \sim Ca^{1/2}$ [19]. We have measured a directly by using IMAGEJ [34], and found it relatively insensitive to shear. In the static foam, $a \approx 0.17R$, which is in close agreement with previous computations [35]. With shearing, a tends to increase with Ω but quickly saturates to an average value of $a \approx 0.2R$ at about 25 rpm. Apparently, the close packing constrains the bubble movement and diminishes the role of shearing. Measuring a among hundreds of pairs of bubbles reveals moderate variations in any given foam, and Fig. 8 shows a typical distribution of a in a sheared foam. Since smaller a gives faster film drainage, and we are concerned with the onset

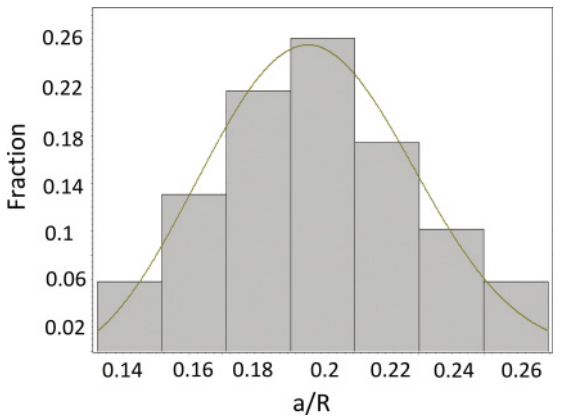

FIG. 8. (Color online) Distribution of the film radius a in a sheared bubble raft with $R = 500\,\mu$m, $\Omega = 75$ rpm. The curve shows a fitted normal distribution.

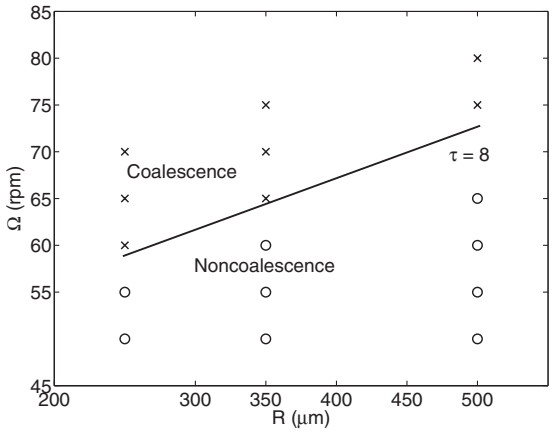

FIG. 9. The critical condition for coalescence corresponds to $\tau = 8$ for solution I, with τ being computed for the innermost layer of bubbles using the measured bubble velocity profile. For solutions II and III, the critical τ values are 12.5 and 28.5, respectively.

of coalescence, we use the smallest $a = 0.14R$. Inserting this value along with Eqs. (7) and (8) into Eq. (6), the ratio between drainage and interaction times is

$$\tau = \frac{t_d}{t_i} = 1.64 \times 10^{-3} \left(\frac{\pi\sigma}{A}\right)^{0.6} \frac{\mu R^{0.2}\dot{\gamma}}{\rho \sum_{i=1}^{N-1} \frac{u^2}{r}}, \qquad (9)$$

where we have neglected h_0^{-2} relative to h_c^{-2}, and taken the interaction time between neighboring rows of bubbles to be $t_i \approx \dot{\gamma}^{-1}$ as in a previous analysis [19]. We argue that $\tau \lesssim O(1)$ should give the critical condition for the anomalous coalescence observed here.

The validity of the scaling theory can now be tested against the key experimental observations. First, note that $\dot{\gamma}$ and u are both proportional to Ω. Thus, $\tau \sim \Omega^{-1}$ and $\tau < 1$ does yield a *minimum* critical rotational speed as observed. Quantitatively, however, the critical condition corresponds to $\tau = 8$, 12.5, and 28.5 for solutions I, II, and III, respectively (Fig. 9). These numbers are one order of magnitude too large. Second, the τ criterion predicts a scaling for the critical rotational speed $\Omega_c \sim R^{0.2}$, which is in reasonable agreement with the power-law scaling observed in Fig. 5. Third, it also predicts Ω_c to increase linearly with the liquid viscosity μ. While the trend is correct, the experimentally observed dependence on μ is much weaker: $\Omega_c \sim \mu^{0.1}$ (cf. Fig. 5). Finally, the large bubbles appear more often in the inner part of the gap than in the outer. Given that the smallest a can be anywhere in a particular experiment, this provides indirect support for the accumulation of the inward force in Eq. (7).

Thus, the inertia-based mechanism explains the qualitative trends observed. But quantitatively it overestimates the drainage time as well as the effect of liquid viscosity. The latter recalls the study of Yoon *et al.* [36] on freely suspended droplets, where the viscosity effect is also weaker than expected. In our case, the numerical discrepancies have many potential causes. For example, the Hamaker constant [33] is not known for the fluids used here, and possibly the bubble surface may develop dimples during thinning [21] that would compromise the calculation above. Since our bulk surfactant concentration is 100 times CMC, the abundance of surfactants may introduce additional effects. Rapid adsorption onto the bubble surface may partially mitigate the Marangoni stress and locally remobilize the surfaces [27]. Though this has been dismissed as a critical condition for the anomalous coalescence, it might explain the fact that the drainage rate is underestimated in our model, producing too large a critical τ value. Moreover, the later stage of drainage is probably influenced by the presence of micelles, which may form layers that hinder film thinning below $h \sim 100$ nm [27]. This nonviscous effect may reduce the overall dependence on μ. Unfortunately, not knowing the chemical properties of the surfactant mixture in the detergent, it is difficult to formulate these ideas quantitatively.

V. CONCLUSION

We have reported an anomalous type of bubble coalescence in a monolayer sheared in a Couette device, which occurs above a critical rotational speed Ω_c. This contrasts with the conventional wisdom about bubble and drop coalescence that it occurs below a critical capillary number. Our coalescence cannot be characterized by a critical capillary number; the critical Ω_c increases with bubble size and the viscosity of the suspending liquid. To rationalize the experimental observations, we have considered three potential mechanisms for the coalescence: shear preventing the formation of surfactant-stabilized films between bubbles, shear stress overcoming Marangoni stress to remobilize the bubble surface, and centripetal force pressing the bubbles radially inward into each other. None of these accounts quantitatively for all of the experimental results.

The third is the most promising. According to this model, the anomalousness of the scenario arises from two factors: the film drainage is driven by a centripetal force instead of a viscous one, and the bubble deformation is determined by geometric constraints rather than shearing. The apparent reversal in the coalescence criterion, from the conventional maximum capillary number to a minimum shear rate, is similar in spirit to that demonstrated recently by Ramachandran and Leal [37] for collision between vesicles. Though clearly not a complete theory for the anomalous coalescence, the inertia-based model captures the qualitative trends of the experiment, and may serve as a starting point for further investigations.

ACKNOWLEDGMENTS

We thank G. M. Homsy, A. Ramachandran, and R. Zenit for helpful discussions. The study was supported by NSERC, the Canada Research Chair program, and the Canada Foundation for Innovation.

[1] J. A. Glazier and D. Weaire, J. Phys. Condens. Matter **4**, 1867 (1992).
[2] N. Vandewalle and J. F. Lentz, Phys. Rev. E **64**, 021507 (2001).
[3] H. Ritacco, F. Kiefer, and D. Langevin, Phys. Rev. Lett. **98**, 244501 (2007).
[4] D. Weaire and N. Rivier, Contemp. Phys. **25**, 59 (1984).

[5] V. Carrier and A. Colin, Langmuir **19**, 4535 (2003).
[6] A.-L. Biance, A. Delbos, and O. Pitois, Phys. Rev. Lett. **106**, 068301 (2011).
[7] G. Debrégeas, H. Tabuteau, and J.-M. di Meglio, Phys. Rev. Lett. **87**, 178305 (2001).
[8] J. Lauridsen, M. Twardos, and M. Dennin, Phys. Rev. Lett. **89**, 098303 (2002).
[9] K. Golemanov, S. Tcholakova, N. D. Denkov, K. P. Ananthapadmanabhan, and A. Lips, Phys. Rev. E **78**, 051405 (2008).
[10] B. Herzhaft, J. Colloid Interface Sci. **247**, 412 (2002).
[11] A. Nandi, A. Mehra, and D. V. Khakhar, Phys. Rev. Lett. **83**, 2461 (1999).
[12] Y. Wang, K. Krishan, and M. Dennin, Phys. Rev. E **74**, 041405 (2006).
[13] G. Katgert, B. P. Tiche, M. E. Mobius, and M. van Hecke, Europhys. Lett. **90**, 54002 (2010).
[14] C. Quilliet, M. Idiart, B. Dollet, L. Berthier, and A. Yekini, Colloids Surf. A **263**, 95 (2005).
[15] R. S. Ghaskadvi and M. Dennin, Rev. Sci. Instrum. **69**, 3568 (1998).
[16] G. K. Batchelor, *An Introduction to Fluid Dynamics*, 3rd ed. (Cambridge University Press, Cambridge, 2000).
[17] A. Chesters and G. Hofman, Appl. Sci. Res. **38**, 353 (1982).
[18] S. G. Yiantsios and R. H. Davis, J. Colloid Interface Sci. **144**, 412 (1991).
[19] A. K. Chesters, Chem. Eng. Res. Des. **69**, 259 (1991).
[20] N. D. Denkov, S. Tcholakova, K. Golemanov, K. P. Ananthapadmanabhan, and A. Lips, Phys. Rev. Lett. **100**, 138301 (2008).
[21] I. U. Vakarelski, R. Manica, X. Tang, S. J. O'Shea, G. W. Stevens, F. Grieser, R. R. Dagastine, and D. Y. C. Chan, Proc. Natl. Acad. Sci. USA **107**, 11177 (2010).
[22] Y. T. Hu, D. J. Pine, and L. G. Leal, Phys. Fluids **12**, 484 (2000).
[23] A. S. Hsu, A. Roy, and L. G. Leal, J. Rheol. **52**, 1291 (2008).
[24] R. A. Medrow and B. T. Chao, Phys. Fluids **14**, 459 (1971).
[25] L. A. Lobo, A. D. Nikolov, A. S. Dimitrov, and P. A. Kralchevsky, Langmuir **6**, 995 (1990).
[26] Y. Yoon, A. Hsu, and L. G. Leal, Phys. Fluids **19**, 023102 (2007).
[27] R. J. Pugh, Adv. Colloid Interface Sci. **64**, 67 (1996).
[28] J. M. Corkill, J. F. Goodman, C. P. Ogden, and J. R. Tate, Proc. R. Soc. London A **273**, 84 (1963).
[29] N. D. Denkov, S. Tcholakova, K. Golemanov, and A. Lips, Phys. Rev. Lett. **103**, 118302 (2009).
[30] V. G. Levich, *Physicochemical Hydrodynamics* (Prentice-Hall, Englewood Cliffs, NJ, 1962).
[31] G. M. MacKay and S. G. Mason, Can. J. Chem. Eng. **41**, 203 (1963).
[32] A. K. Chesters and I. B. Bazhlekov, J. Colloid Interface Sci. **230**, 229 (2000).
[33] J. N. Israelachvili, *Intermolecular and Surface Forces*, 2nd ed. (Academic, London, 1991).
[34] W. S. Rasband, computer code IMAGEJ (National Institutes of Health, Bethesda, MD, 1997-2012), [http://rsb.info.nih.gov/ij/].
[35] S. J. Cox and E. Janiaud, Philos. Mag. Lett. **88**, 693 (2008).
[36] Y. Yoon, M. Borrel, C. C. Park, and L. G. Leal, J. Fluid Mech. **525**, 355 (2005).
[37] A. Ramachandran and G. Leal, Phys. Fluids **22**, 091702 (2010).